

Using Density Evolution for Analysis of Low Complexity MIMO Detector based on Belief Propagation over a Ring Type Pair-wise Graph

Seokhyun Yoon¹

¹ Department of Electronics & Electrical Engineering, Dankook University
126 Jukjeon-dong, Suji-gu, Yongin-si, Gyeonggi-do, 440-701, Republic of Korea
E-mail: ¹syoon@dku.edu

Abstract: The convergence and density evolution of a low complexity MIMO detection based on belief propagation over a ring-type pair-wise graph is considered for binary input. The algorithm has been originally proposed in [1], where the convergence for Gaussian input have been analyzed. Here, we extend the convergence analysis to binary data and provide an asymptotic performance in terms of BER and SINR via density evolution analysis.

1. Detection Algorithm

System Model: A Gaussian MIMO system with a constant $N \times M$ channel matrix \mathbf{H} ($N \geq M$) is modeled by

$$\mathbf{y} = \mathbf{H}\mathbf{x} + \mathbf{n} = \sum_{k=1}^M \mathbf{h}_k x_k + \mathbf{n} \quad (1)$$

where \mathbf{x} is $M \times 1$ transmitted data symbol vector, \mathbf{n} is $N \times 1$ noise vector, \mathbf{y} is $N \times 1$ received signal vector and \mathbf{h}_m is the m th column of \mathbf{H} . \mathbf{n} is assumed to be complex Gaussian with mean $\mathbf{0}$ and covariance $E[\mathbf{nn}^H] = \sigma^2 \mathbf{I}$. Each element of \mathbf{x} is usually a 2^m -ary symbol drawn from a finite alphabet set Ξ of size 2^m , such as QPSK or 16QAM.

Detection algorithm: Our start point is the one in [1], especially the BP over the ring-type pair-wise graph, for which the algorithm effectively a forward-backward recursion. The graphical model is shown in Fig.1, over which the BP algorithm is summarized as follows. BP over the ring-type pair-wise graph (Forward-backward recursion) [1]: Given the messages in the previous iteration, $\pi_{k \rightarrow i}(x_i)$, it is recursively updated for all j as

$$\pi_{j \rightarrow (j \pm 1)_M}(x_{j \pm 1}) = \sum_{x_j \in \Xi} \tilde{p}(x_{(j \pm 1)_M} | x_j, y_{(j \pm 1)_M}) \cdot \pi_{(j \mp 1)_M \rightarrow j}(x_j) \quad (1)$$

The message update is repeated by a pre-defined number or until the messages do not change any more and, finally, the belief is obtained by

$$b(x_j) = \pi_{(j+1)_M \rightarrow j}(x_j) \cdot \pi_{(j-1)_M \rightarrow j}(x_j) \quad (2)$$

In (1) and (2), $(\cdot)_M$ is one-base modulo- M operation. Since it is awkward to use every time, we will omit it later on. In this algorithm we used only factor to variable node message, $\pi_{k \rightarrow i}(x_i)$, since there is only two factor nodes connected to a variable node such that variable nodes simply pass the incoming message to the opposite side. In (2), the translation function, $\tilde{p}(x_{(j \pm 1)_M} | x_j, y_{(j \pm 1)_M})$, is based on the conditional MMSE estimator of x_j given $x_{j \pm 1}$. Defining the conditional MMSE estimator of x_j given x_i as $\mathbf{w}_{ji} = \mathbf{K}_{\{j,i\}}^{-1} \mathbf{h}_j$ and applying it to the received signal vector \mathbf{y} , we have

$$y_{ji} = \mathbf{w}_{ji}^H \mathbf{y} = a_{ji,j} x_j + a_{ji,i} x_i + n_{ji} \quad (3)$$

This research was supported by the MSIP(Ministry of Science, ICT and Future Planning), Korea, under the ITRC(Information Technology Research Center) support program (IITP-2016-R0992-16-1012) supervised by the IITP(Institute for Information & communications Technology Promotion)

where

$$\mathbf{K}_{\Phi} = \sigma^2 \mathbf{I} + \sum_{k \in \Phi} \mathbf{h}_k \mathbf{h}_k^H \quad (5)$$

$$a_{ji,k} = \mathbf{w}_{ji}^H \mathbf{h}_k = \mathbf{h}_j^H \mathbf{K}_{\{j,i\}}^{-1} \mathbf{h}_k \quad \text{for } k = i \text{ or } j \quad (6)$$

$$E |n_{ji}|^2 = \mathbf{w}_{ji}^H \mathbf{K}_{\{j,i\}} \mathbf{w}_{ji} = \mathbf{h}_j^H \mathbf{K}_{\{j,i\}}^{-1} \mathbf{h}_j \equiv \sigma_{ji}^2 \quad (7)$$

Note that $\sigma_{ji}^2 = a_{ji,j}$. In the truncated signal model in (4), we assume the noise + interference, n_{ji} , to be a Gaussian, from which the translation function is given by

$$\tilde{p}(x_j | x_i, y'_{ji}) \propto \tilde{p}(y'_{ji} | x_i, x_j) p(x_j) \quad (8)$$

with

$$\tilde{p}(y'_{ji} | x_i, x_j) = \mathcal{CN}(y'_{ji}; a_{ji,j} x_j + a_{ji,i} x_i, \sigma_{ji}^2) \quad (9)$$

where ‘ \sim ’ on top of the conditional functions in (8) and (9) indicate that they are given by Gaussian density and $\mathcal{CN}(x; a, b)$ mean the complex Gaussian density with mean a and variance b .

2. Convergence for Binary Input

2.1 Message passing for binary input

For binary input, the message can be summarized by a scalar, i.e., the LLR. Define the message and *a priori* LLR as

$$l_{k \rightarrow i} = \log \frac{\pi_{k \rightarrow i}(x_i = +1)}{\pi_{k \rightarrow i}(x_i = -1)} \quad (14)$$

$$l_{a,i} = \log \frac{p(x_i = +1)}{p(x_i = -1)}$$

Then, the forward recursion in (2), together with (14), can be expressed as

$$l_{j-1 \rightarrow j} = l_{a,j} + 4y_{j|j-1} - \zeta(l_{j-2 \rightarrow j-1} + 2d_{j|j-1}; c_{j|j-1}) \quad (16)$$

Where the function $\zeta(x; c)$ of x with a parameter c as

$$\zeta(x; c) \equiv -\log \left(\frac{e^{x/2-c} + e^{-x/2+c}}{e^{x/2+c} + e^{-x/2-c}} \right), \quad (17)$$

and

$$y_{ji}^{(R)} = \text{Re}[y_{ji}] \quad (19)$$

$$c_{ji} = \frac{2}{\sigma_{ji}^2} \text{Re}[a_{ji,j}^* a_{ji,i}] = 2 \text{Re}[a_{ji,i}] = 2a_{ji,i}^{(R)} \quad (20)$$

$$d_{ji} = \frac{2}{\sigma_{ji}^2} \text{Re}[a_{ji,i}^* y_{ji}] \quad (21)$$

where we denote the real and imaginary part of a complex variable as superscript (R) and (I) , respectively, for notational simplicity. The non-linear function $\zeta(x; c)$ in (17) has the following properties.

- i) $\zeta'(x; c) = \frac{d}{dx} \zeta(x; c) = \frac{1}{2} \tanh\left(\frac{x}{2} + c\right) - \frac{1}{2} \tanh\left(\frac{x}{2} - c\right)$
- ii) $|\zeta'(x; c)| < 1 \quad \forall x$ (obvious from i))

- iii) $\zeta(x; c)$ is a monotonic function of x . (either increasing if $c > 0$ or decreasing if $c < 0$)
- iv) $\lim_{x \rightarrow \pm\infty} \zeta(x; c) \rightarrow \pm 2c$ (Saturation)
- v) $\lim_{c \rightarrow 0 \pm} \frac{1}{2c} \zeta(x; c) \rightarrow \tanh\left(\frac{x}{2}\right)$

2.2 Convergence Proof

We first consider the following lemma.

Lemma 1: Let $f(x)$ be a function with the following two properties

- i) $f(x)$ is a monotonic (either increasing or decreasing) function defined on $(-\infty, \infty)$.
- ii) $|f'(x)| < 1 \forall x$, where $f'(x) = df(x)/dx$.

Then, the followings hold

- iii) The equation, $f(x) = x$, has a unique solution.
- iv) Let x_s be the solution of $f(x) = x$. Let x_k for $k = 1, 2, 3 \dots$ be a sequence obtained by successively applying f starting from an initial value x_0 , i.e., $x_k = f(x_{k-1})$. Then, for any x_0 , x_k approaches to x_s as $k \rightarrow \infty$.
- v) Let $g(x) = cf(x-a)+b$ for some real values a and b and $-1 \leq c \leq +1$. The properties i) to iv) also hold for $g(x)$.

From *lemma 1*, one can prove the convergence of the forward-backward recursion for binary input as follows.

Theorem 2: The forward and backward recursion in (18) for binary input converges to a unique fixed point as iteration goes to infinity.

3. Density Evolution Analysis

Assuming the channel matrix \mathbf{H} and the noise power σ^2 are fixed and the channel is used many times across a codeword, we develop the density evolution of messages between neighboring nodes. In channel coding context, the density evolution in an iterative decoder assumes all-zero sequence is sent and the LLR mean is tracked with the number of iterations, assuming the LLR is Gaussian with its variance being the same as its mean. The density evolution used in channel decoding assumes the same, even though the approach is different. In this section, we will also assume the LLRs are Gaussian and will track their mean and variance. The differences here from those in iterative channel decoding are that 1) the mean and variance have to be tracked along the ring, where the message of each node has different statistics and, hence, 2) we cannot assume all-zero input since the statistics of the current message, $l_{j-1 \rightarrow j}$, depends not only on the background noise but also on the other data. Fortunately, symmetry holds for binary data and the message depends largely on the previous data only so that one can proceed as follows: Under symmetry, we denote the mean and variance of $l_{j-1 \rightarrow j}$ as $m_{j|j-1}x_j$ and $v_{j|j-1}$, where both $m_{j|j-1}$ and $v_{j|j-1}$ are non-negative and the mean $m_{j|j-1}x_j$ has the same sign as that of x_j . In this definition, $m_{j|j-1}$ can be interpreted as a reliability of $l_{j-1 \rightarrow j}$. Then, supposing that $x_j = +1$, we evaluate $(m_{j|j-1}, v_{j|j-1})$ for given $(m_{j-1|j-2}, v_{j-1|j-2})$ by averaging over all possible combination

of x_{j-1} , $\mathbf{x}_{\setminus\{j,j-1\}}$ (\mathbf{x} excluding x_j and x_{j-1}) and \mathbf{n} . Due to page limitation, we omit the details of the density evolution.

4. Numerical Results

Fig.1 compares the BER curves obtained via density evolution and its lower bound obtained by the SINR bound in (47) with that obtained by simulation, which is the same as those in [1] without channel coding. The figure shows that (1) the BER obtained via density evolution matches perfectly to the simulation results and (2) the BER bound is quite tight showing the estimation error from the previous/next nodes has negligible effect especially for binary input. Fig.2 shows the average SINR averaged over the same set of random channels, where one can see that approximately 1.7 dB SINR gain over MMSE receivers.

References

- [1] S. Yoon, "A Low Complexity MIMO Detection Based on Pair-wise Markov Random Fields," Proc. of IEEE VTC 2011 Spring, Budapest, Hungary, May 2011
- [2] S. Yoon and C.-B. Chae, "Low Complexity MIMO Detection Based on Belief Propagation over Pair-wise Graphs," IEEE Trans. on Veh. Tech., Vol.63, No.5, pp.2363-2377, June 2014.
- [3] S.-J. Yoon, J. Lee and S. Yoon, "Performance of MIMO Detectors with a Capacity-Approaching Code," to appear in Proc. of Int'l. Conf. on ICT Convergence 2015 (ICTC 2015), Jeju, Korea, Oct., 2015.

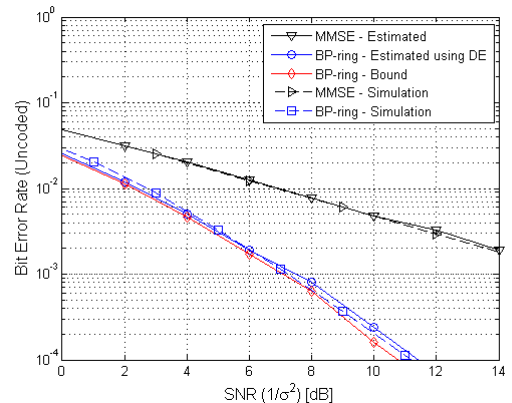


Fig.1 Bit error rate performance

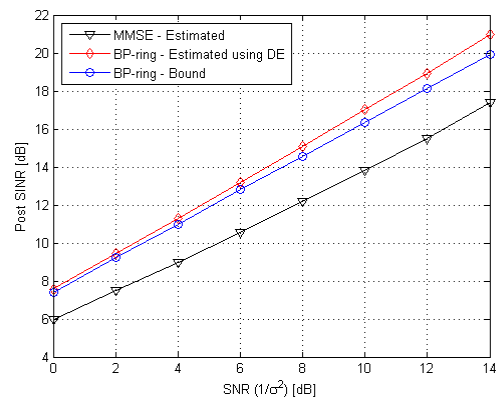


Fig.2 Average SINR